Proc. Natl. Acad. Sci. USA
Vol. 86, pp. 4402–4406, June 1989
Biochemistry

Metabolite specific proton magnetic resonance imaging

(selective coherence transfer/lactic acid/spectral editing)

RALPH E. HURD* AND DOMINIQUE M. FREEMAN

General Electric NMR Instruments, 255 Fourier Avenue, Fremont, CA 94539

Communicated by John D. Roberts, March 9, 1989

ABSTRACT **An imaging method is described that makes use of proton double quantum nuclear magnetic resonance (NMR) to construct images based on selected metabolites such as lactic acid. The optimization of the method is illustrated *in vitro*, followed by *in vivo* determination of lactic acid distribution in a solid tumor model. Water suppression and editing of lipid signals are such that two-dimensional spectra of lactic acid may be obtained from a radiation-induced fibrosarcoma (RIF-1) tumor in under 1 min and lactic acid images from the same tumor in under 1 hr at 2.0 T. This technique provides a fast and reproducible method at moderate magnetic field strength for mapping biologically relevant metabolites.**

This paper describes an efficient proton nuclear magnetic resonance (NMR) imaging method that can be used to noninvasively map the distribution and levels of certain biologically significant metabolites *in vivo*. Metabolites of clinical interest include lactic acid (1), *N*-acetylaspartate (2), alanine (3), and taurine (4). Lactate was chosen for these initial studies because of its biochemical and pathological importance. An elevated level of tissue lactate may indicate (*i*) the presence of hypoxia, characterized by an increased rate of anaerobic glycolysis, as is found in certain solid tumor centers; (*ii*) conditions of reduced blood flow (ischemia), such as occurs in coronary infarct and cerebral stroke; (*iii*) certain inborn errors of metabolism—for example, pyruvate dehydrogenase and pyruvate carboxylase deficiency, or (*iv*) diabetes (type I)—in which oral phenformin overdose might be implicated.

To generate an *in vivo* proton magnetic resonance image based on a metabolite such as lactate requires the elimination, or reduction, of signals from the large population of water and lipid protons present *in vivo*, as well as separation of metabolites, residual water, and residual lipid signals. Because metabolite concentrations and magnetic field strength are the limiting factors for *in vivo* studies, the method must maintain a high level of efficiency in terms of selectivity, sensitivity, and minimum data acquisition time. In a previous study (5), two-dimensional double quantum coherence transfer spectroscopy (Fig. 1*A*) was used to determine steady-state lactate levels *in vivo* (Fig. 1*B*). Because of high residual water and lipid levels observed in data collected by the method shown in Fig. 1, both the double quantum (ω_1) and chemical shift (ω_2) dimensions are needed for spectral editing. This means that a four-dimensional matrix would be required to obtain an image based on this method.

For practical *in vivo* imaging, the aim was to eliminate the requirement for the chemical shift (ω_2) dimension by improving the performance of the double quantum method. The ω_2 dimension can then be used for encoding space rather than chemical shift.

The efficiency and limits of detection of double quantum coherence methods were evaluated by using aqueous solutions of lactic acid or its NMR analogue *N*-acetyl alanine. Metabolite specific images using the technique optimized for water and lipid suppression were then obtained of the lactic acid distribution in radiation-induced fibrosarcoma (RIF-1) tumors implanted in C3H mice.

METHODS

These studies were carried out on a General Electric NMR Instruments 2.0-T CSI spectrometer/imager (Fremont, CA) operating at a proton frequency of 85.56 MHz and equipped with Acustar self-shielded gradients.† Data were collected using a 4-turn 2-cm-diameter solenoid radiofrequency coil.

In the proposed proton double quantum imaging sequence, the t_1 dimension alone is used to discriminate lactate from residual water. Fourier transformation of the t_1 dimension (as few as 16 0.5-msec increments) leads to a relatively broad frequency response. The requirements for water suppression are therefore more stringent, such that the resulting wings of the residual water signal must not extend with significant intensity into the double quantum frequency for lactate. To improve the performance of the double quantum experiment, and thus provide the necessary basis for metabolite specific imaging, three modifications to the basic sequence—(*i*) composite gradients, (*ii*) symmetric multiple quantum excitation/detection (6, 7), and (*iii*) selective coherence transfer—were investigated by obtaining spectra on a 0.5-ml sample of 100 mM *N*-acetyl alanine in water. In addition, pulse-and-acquire and double quantum coherence spectra were performed on a sample in ^2H_2O to determine relative efficacy.

The optimized sequence was then tested *in vivo* in RIF-1 (8). The average tumor size examined was 1.1 g (14 days after implantation). The mice were anesthetized for the duration of the experiment with sodium pentobarbital (70 mg/kg). Animals were placed prone in a Plexiglas holder and a 20-mm 4-turn solenoidal radiofrequency coil was positioned around the tumor. A series of spectra were obtained where the double quantum evolution time (t_1) was incremented in 64 0.5-msec steps from 8 to 40 msec. Each increment was a single acquisition with a 1-sec recycle time. Total acquisition time was 64 sec. The transmitter was set on the α-methine of the lactic acid resonance at 4.2 ppm, and a non-phase-shifted 1331 pulse was used to selectively excite this resonance. The double quantum coherence transfer selection gradients were each 3 msec half sinusoidal with maxima of 3.375 and 6.75 G/cm, respectively.

After the *in vivo* NMR experiments, tumors were freeze-clamped, ground to a fine powder, extracted into cold perchloric acid, and assayed enzymatically for lactic acid (9).

The lactic acid editing sequence was then converted to a proton double quantum imaging sequence (by addition of phase and frequency encoding gradients). The limit of de-

The publication costs of this article were defrayed in part by page charge payment. This article must therefore be hereby marked "*advertisement*" in accordance with 18 U.S.C. §1734 solely to indicate this fact.

Abbreviation: RIF-1, radiation-induced fibrosarcoma.

*To whom reprint requests should be addressed.

†Roemer, P. B., Edelstein, W. A. & Hickey, J. S., Fifth Annual Meeting of the Society of Magnetic Resonance in Medicine, Aug. 19–22, 1986, Montreal, pp. 1067–1068.

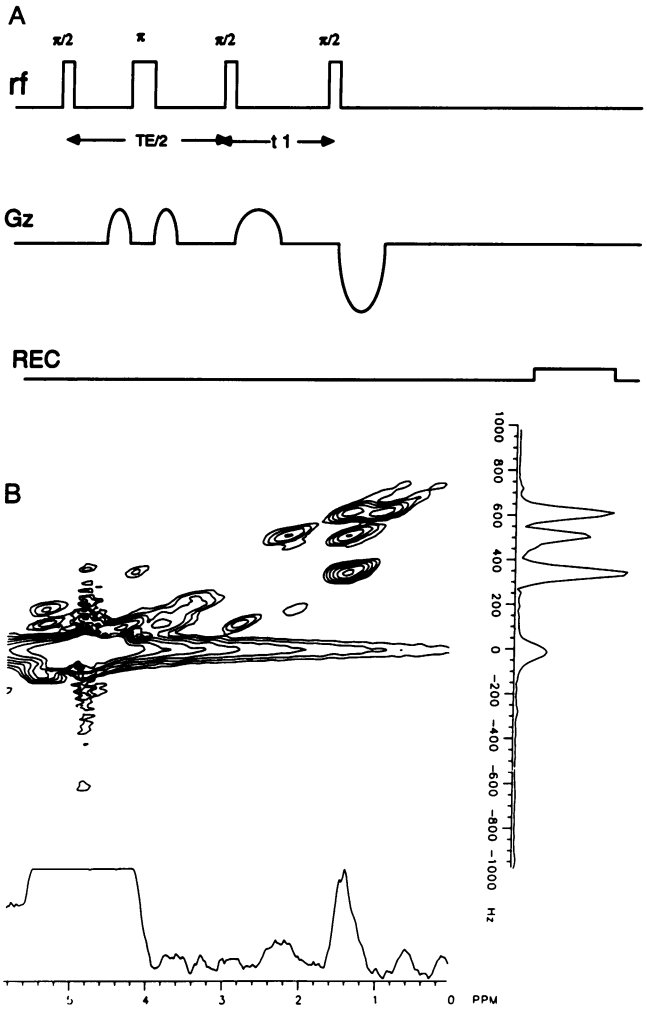

FIG. 1. (*A*) Two-dimensional double quantum coherence transfer sequence. The three time lines indicate radiofrequency (rf), the z gradient (Gz), and the receiver gate (REC). The total echo time (TE) is set to 68 msec for these experiments. (*B*) Contour plot of a two-dimensional double quantum coherence transfer experiment (using the sequence shown in *A*) performed *in vivo* on a RIF-1 tumor implanted on the back of a C3H mouse. This 34-min lactate edited spectrum was collected as a 64 × 2K matrix covering 2000 Hz in ω_1 and 5000 Hz in ω_2. The ω_1 dimension (double quantum frequency axis) was created by allowing t_1 to evolve in 0.5-msec steps from 10 to 42 msec. The transmitter was set to the water resonance frequency (4.7 ppm). Sixteen acquisitions, with a 1-sec recycle time, were acquired for each t_1 increment. The one-dimensional spectrum on the chemical shift axis (ω_2) is the first block of the two-dimensional array. The spectrum on the double quantum axis (ω_1) was extracted from the two-dimensional array at 1.3 ppm. A 16-step phase cycle was used as described (5). The lactic acid signal corresponds to 8.17 μmol/g (wet weight) of tumor. The tumor weight was 1.16 g.

tection of this imaging sequence was determined in a phantom consisting of three 5-mm-diameter tubes containing 2.5, 5, and 10 mM lactate in water, placed in a 12-mm tube containing water. Data were collected as a three-dimensional matrix consisting of 16 t_1 increments, 64 phase encode steps, and 128 complex frequency encode points. These images were acquired in under an hour with 2 acquisitions per block and a 1.5-sec recycle time. The field of view was 10 cm, and the transmitter was set at the lactate methyl resonance. A frequency selective $1\bar{3}3\bar{1}$ pulse with a 2-msec interpulse delay was used to selectively excite the lactate methine. Data were zero-filled once in the phase encode dimension and then processed by three-dimensional Fourier transformation. Lactate solutions were assayed spectrophotometrically to confirm concentration.

Lactic acid images (using the same parameters as described above) were then obtained immediately postmortem in a mouse bearing a RIF-1 tumor. These results were used for comparison with lactic acid images obtained from a live anesthetized mouse bearing a RIF-1 tumor of the same size.

RESULTS

Residual water signal was significantly reduced using a composite (simultaneous *x*, *y*, and *z*) gradient pair to select for double quantum coherence transfer (compare Fig. 2 *A* and *B*). This leaves the water spins dephased along the vector sum of the three orthogonal gradients, rather than along only one primary gradient axis, and thereby diminishes the probability of unwanted water signal being rephased by a spurious gradient during acquisitions.

Signal was increased by ≈40% using a symmetric multiple quantum excitation/detection rf scheme (6, 7) (compare Fig. 2 *C* with *B*). However, we have found that an even greater increase in efficiency is achieved by generating selective coherence transfer (compare Fig. 2 *D* with *B*). If a frequency-selective rf pulse is used in place of the third $\pi/2$ pulse to selectively excite the α-methine at 4.2 ppm, optimum coherence transfer from methine to methyl is observed.

Selective coherence transfer should theoretically give a factor of 2 improvement over the coherence transfer experiment with a nonselective $\pi/2$ pulse. Nonselective coherence transfer signal intensity varies as $\sin\alpha\cos^2(\alpha/2)$, where α is the tip angle of the third read pulse (10). The selective version varies as $\sin\alpha$ (R. Freeman, personal communication). This dependence was also experimentally verified (data not shown). Any selective $\pi/2$ pulse that excites the methine signal and not the methyl will produce similar results. For binomial type sequences (11, 12), the maximum should be set at the frequency of the α-methine and the null at the β-methyl. The ultimate consequence of choosing a selective rf pulse in which the transmitter is set off-resonance, at the desired null frequency (e.g., $1\bar{1}$ or $1\bar{3}3\bar{1}$), rather than on-resonance (e.g., 11, 1331, or a truncated $\sin x/x$), is that residual water will be observed near 600 Hz rather than around −100 Hz in the (ω_1) frequency dimension. In this implementation, the transmitter is set at the frequency of one of the lactate resonances, and, as such, the lactate resonance will be observed at a double quantum frequency of 250 Hz at 2.0 T.

The selective coherence transfer also serves to reduce lipid signals overlapping the lactate methyl resonance in the region of 1.4 ppm since selective excitation of the lactate methine at 4.2 ppm does not appreciably excite these lipid resonances.

The efficiency of the sequence shown in Fig. 2*D* (for lactate methyl signal to noise) was determined to be ≈50% relative to a simple $\pi/2$ pulse-and-acquire spectrum of lactate in 99.5% ^2H_2O (data not shown). The ^2H_2O was used to eliminate any dynamic range limitation for the ideal pulse-and-acquire measurement.

The combination of selective coherence transfer, symmetric two-dimensional multiple quantum excitation/detection, and the use of composite gradients promises to yield the most effective lactate editing. The selective coherence transfer results in a single (CH_3) resonance detected for lactate and thereby prevents a chemical shift artifact that would arise from the lactate methine in the imaging experiment.

The sequence shown in Fig. 2*D* was tested *in vivo* to obtain a lactate edited proton two-dimensional NMR spectrum of a RIF-1 tumor implanted in a live anesthetized C3H mouse (Fig. 3). These results are directly comparable to those shown in Fig. 1*B* and clearly illustrate *in vivo* the optimizations described in Fig. 2.

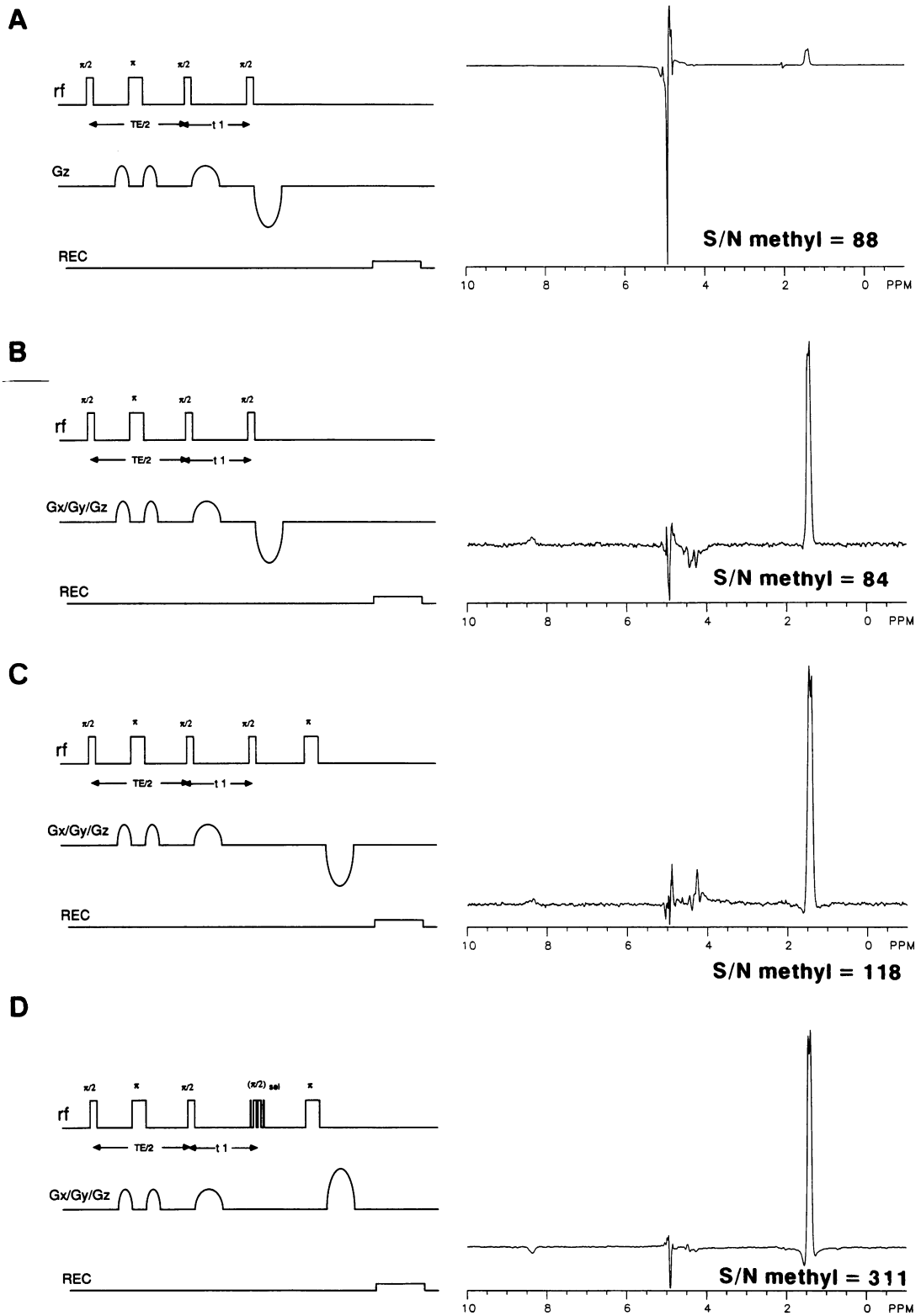

FIG. 2. The optimization of the proton double quantum sequence. The sample used to compare sequences was 0.5 ml of a 100 mM *N*-acetylalanine solution. This provided a suitable NMR analogue for the AX_3 spin system in lactic acid. For this study, all system variables were held constant (gain, spectral width, and a single acquisition). Pulse sequences, experimental spectra, and measured signal/noise ratios (S/N) are shown left to right for each of the four sequences. (*A*) The basic double quantum coherence sequence. (*B*) Same as in *A* but with composite gradients in *x*, *y*, and *z*. (*C*) The use of a symmetric excitation/detection rf sequence. (*D*) The addition of selective coherence transfer.

In addition, a dramatic reduction in data acquisition time was realized as a result of the refinements. Because of water suppression efficiency and lactate signal level, only a single acquisition per t_1 increment was necessary. Elimination of the phase cycling and signal averaging requirement decreased data acquisition from >30 min to just over 1 min (64 t_1 values with a 1-sec recycle time) for the spectrum shown in Fig. 3. Potentially, only 16 t_1 steps (or 16 sec) would be required for

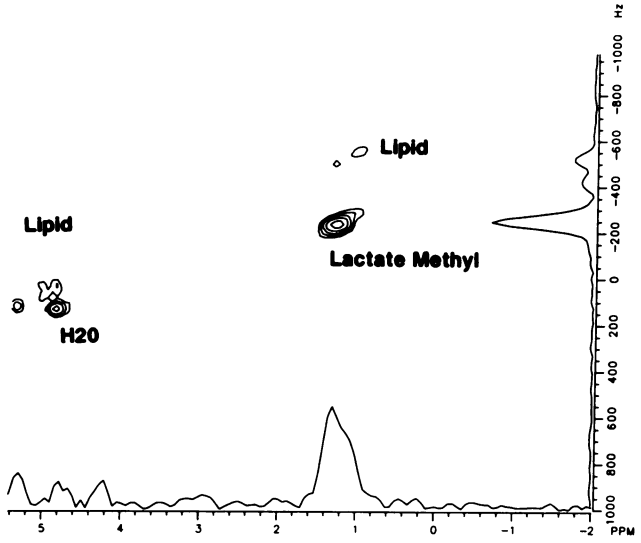

FIG. 3. Contour plot of a proton double quantum experiment, performed *in vivo*, on a RIF-1 tumor implanted on the back of a C3H mouse. This 64-sec lactate spectrum was acquired as a 64 × 2K matrix covering 2000 Hz in ω_1 and 5000 Hz in ω_2. The ω_1 dimension (double quantum frequency axis) was created by allowing t_1 to evolve in 0.5-msec steps from 8 to 40 msec. TE was set to 68 msec. The transmitter was set to the lactate methine resonance frequency (4.2 ppm) and a non-phase-shifted 1331 pulse was used to selectively excite this resonance. A single acquisition, with a 1-sec recycle time, was collected for each t_1 increment. The one-dimensional spectrum on the chemical shift axis (ω_2) is the first block of the two-dimensional array. The spectrum on the double quantum axis (ω_1) was extracted from the two-dimensional array at 1.4 ppm.

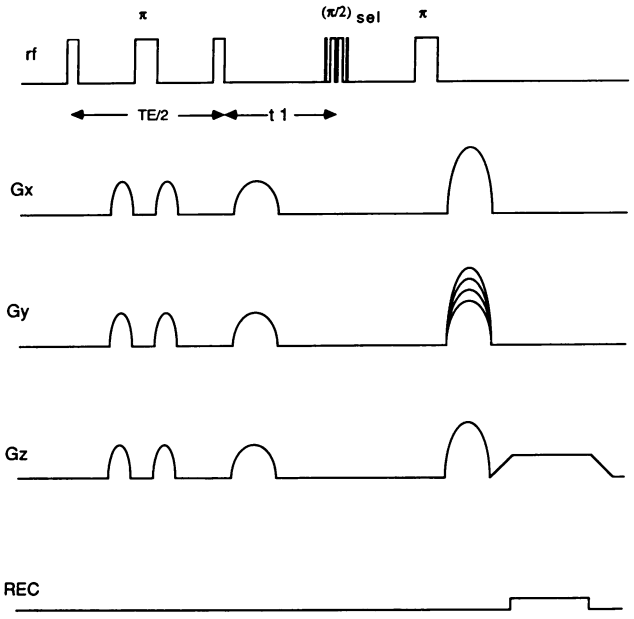

FIG. 4. Proton double quantum lactate imaging sequence.

Fourier transformation to discriminate lactate from the residual lipid signals. Lactate level in this study was enzymatically determined to be 10 μmol/g (wet weight) of tumor tissue.

The proton double quantum editing sequence shown in Fig. 2*D* was converted to a proton double quantum imaging sequence by addition of phase encoding and frequency encoding gradients (Fig. 4). To determine the limit of detection of this method, an image was obtained of a phantom containing three different concentrations of lactic acid (Fig. 5*B*). The lactate image was extracted as a 128 × 128 matrix at the lactate double quantum frequency (ω_1 = 250 Hz) and is shown with a normal proton image for comparison in Fig. 5*A*.

Using this sequence, an "*in vivo*" lactate image was obtained immediately postmortem on an implanted RIF-1 tumor. Fig. 6*A* shows the normal T_2-weighted proton image. The image represents the distribution of the lactic acid throughout the volume of the tumor. Delineation of tumor from normal tissue as well as from the bone marrow in the femur is shown. Proton double quantum NMR images were obtained by using the parameters described above. The lactate image at the double quantum frequency of 250 Hz (see Fig. 6*B*) manifests a heterogeneous distribution of lactate in the tumor and a larger homogeneous distribution of lactate in the tissue surrounding the tumor (mostly skin and muscle). Fig. 6*C* represents the image at 0 Hz, the double quantum frequency for residual lipid under these conditions. Superimposing this image on the proton image in Fig. 6*A* indicates that this corresponds to the bone marrow of the mouse femur.

The metabolite specific imaging protocol was repeated on two live anesthetized C3H mice bearing RIF-1 tumors. The *in vivo* results also showed a heterogeneous distribution of lactate attributed to islands of hypoxic cell activity. Unlike the postmortem example, no lactate signal was observed from normal tissue (Fig. 7). Enzymatic assay indicated an average lactate concentration of 12 μmol/g (wet weight) for the tumor shown in Fig. 7.

DISCUSSION

Selective two-dimensional double quantum coherence transfer provides the editing and water suppression required for *in*

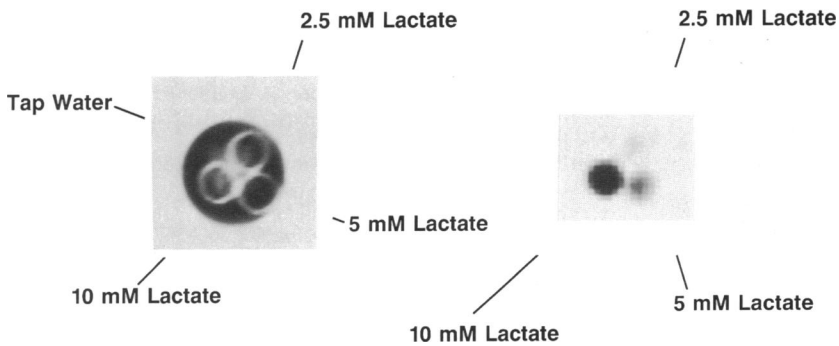

FIG. 5. *In vitro* lactate imaging. (*A*) Normal proton image with a recycle time (TR) = 1500 msec, and an echo time (TE) = 28 msec. (*B*) Lactate image obtained using the sequence shown in Fig. 4, in a phantom consisting of three 5-mm-diameter tubes containing 10 mM lactate, 5 mM lactate, and 2.5 mM lactate placed in a 12-mm-diameter cylinder containing tap water. TR = 2000 msec, TE = 68 msec. These data were acquired and processed as described in the text.

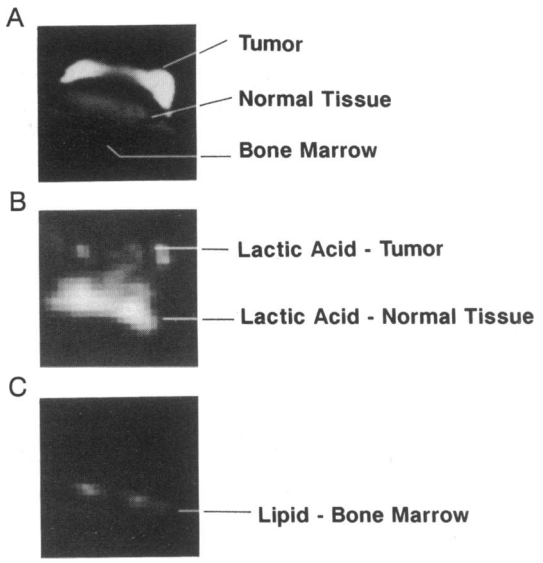

FIG. 6. Proton double quantum images obtained immediately postmortem on a RIF-1 tumor implanted on the back of a C3H mouse. Data were collected with a total acquisition time of 51 min for a 16 × 64 × 128 array. The images shown are normal T_2 weighted proton image (TR = 1500 msec, TE = 50 msec) of the tumor (*A*); lactate image showing heterogeneous distribution of lactate in tumor and homogeneous distribution of lactate in surrounding tissue (*B*); lipid image, primarily bone marrow in femur (*C*).

vivo metabolite-specific spectroscopy and imaging. The advantages of this method over conventional editing sequences (13–16) are that it is not a difference method and therefore is not subject to motion- and stability-related subtraction errors, and it provides an optimum level of efficacy for lactic acid.

As a spectroscopic technique, it provides a fast (<1 min) reliable measurement of lactate levels *in vivo*. As an imaging method, the technique is capable of detecting pathologically relevant levels of lactic acid, of the order of 2.5 mM, at a moderate field strength (2.0 T). Good spatial detail, ≈20 μl/voxel, observed in these projection images can be readily achieved. The technique performs well even in the presence of large lipid concentrations and consequently is not limited to use in regions of interest that are low in "NMR visible" lipid, such as brain. This avoids having to make the assumption that pathology or reduction in blood flow or oxygen tension does not render the lipid components in these regions more mobile and hence NMR visible. In fact, the assumption that lipid components of tissue remain unchanged structurally during hypoxia or ischemia can be dangerous (17) since certain membrane changes have been documented in reduced blood flow (18).

Volume selective and spectroscopic imaging versions of this technique are readily constructed to meet specific *in vivo* applications. Slice-selective imaging is possible by utilizing the final π pulse to define the slice. One remaining aspect is the determination of absolute concentrations of metabolites by NMR. Noninvasive characterization of extent and severity of the biochemical changes occurring prior to and during treatment would provide an important clinical tool for gauging response to tumor therapy.

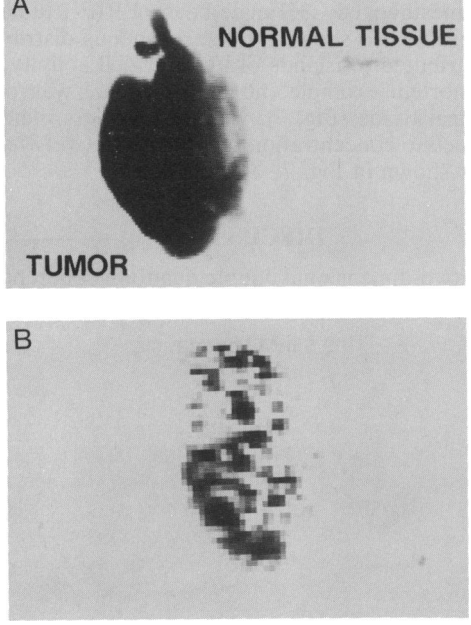

FIG. 7. *In vivo* proton double quantum lactate image of a RIF-1 tumor implanted on the back of a live anesthetized C3H mouse. Data were acquired as described for Fig. 6. The images shown are a normal T_2 weighted proton image of tumor (TR = 1500 msec, TE = 50 msec) (*A*) and lactate image showing heterogeneous distribution of lactate in tumor (*B*). No lactate was observed in the surrounding tissue.

The authors are grateful to Ray Freeman, Xi-Li Wu, and Helen Geen (University of Cambridge, Cambridge, U.K.) for discussions on theoretical aspects of the selective double quantum experiment. The authors wish to thank Holde Muller (Department of Diagnostic Radiology, Stanford University School of Medicine) and Marilyn Lemmon (Department of Therapeutic Radiology, Stanford University Medical Center) for supplying the RIF-1 tumors. We thank Karen Corbett for preparation of the manuscript.

1. Warburg, D. (1956) *Science* **124,** 269–274.
2. Crockard, H. A., Gadian, D. G., Frackowiak, R. S. J., Proctor, E., Allen, K., Williams, S. R. & Russell, R. W. R. (1987) *J. Cereb. Blood Flow Metab.* **7,** 394–398.
3. Ross, B. D. (1988) in *New Aspects of Renal Ammonia Metabolism*, eds. Barbarel, G., Schoolworth, A. C., Endon, H., Rengel, M. & Tizianello, A. (Karger, New York), Vol. 63, pp. 53–59.
4. Evanochko, W. T., Sakai, T. T., Ng, T. C., Krishna, N. R., Kim, H. D., Zeidler, R. B., Ghanta, V. K., Brockman, K. W., Schiffer, L. M., Braunschweiger, P. G. & Glickson, J. D. (1984) *Biochim. Biophys. Acta* **805,** 104–116.
5. Sotak, C. H., Freeman, D. M. & Hurd, R. H. (1988) *J. Magn. Reson.* **78,** 355–361.
6. Sorensen, O. W., Levitt, M. H. & Ernst, R. R., (1983) *J. Magn. Reson.* **55,** 104–113.
7. Rance, M., Sorensen, O. W., Leupin, W., Kogler, H., Wutrich, K. & Ernst, R. R. (1985) *J. Magn. Reson.* **61,** 67–80.
8. Twentyman, P. R., Brown, J. M. & Gray, J. W. (1980) *J. Natl. Cancer Inst.* **64,** 595–604.
9. Hohorst, H. J., Kreutz, S. H. & Bucher, T. (1959) *Biochem. Z.* **18,** 332–338.
10. Mareci, T. H. & Freeman, R. (1982) *J. Magn. Reson.* **48,** 158–163.
11. Hore, P. J. (1983) *J. Magn. Reson.* **55,** 283–300.
12. Plateau, P. & Guéron, M. (1982) *J. Am. Chem. Soc.* **104,** 7310–7314.
13. Hardy, C. J. & Dumonlin, C. L. (1987) *Magn. Reson. Med.* **5,** 58–66.
14. Williams, S. R., Gadian, D. G. & Proctor, E. (1986) *J. Magn. Reson.* **66,** 560–567.
15. Rothman, D. L., Arias-Mendoza, F., Shulman, G. I. & Shulman, R. A. (1980) *J. Magn. Reson.* **60,** 430–436.
16. Sotak, C. H. & Freeman, D. M. (1988) *J. Magn. Reson.* **77,** 383–388.
17. Chang, L. H., Pereira, B. M., Weinstein, P. R., Keniry, M. A., Murphy Boesch, J., Litt, L. & James, T. L. (1987) *Magn. Reson. Med.* **4,** 575–581.
18. Vink, R. A., McIntosh, T. K. & Faden, A. I. (1988) *Magn. Reson. Med.* **7,** 95–99.